



Research Article

A novel underactuated exoskeleton rehabilitation glove for hand flexion and extension training

Lei Zhao^a, Fenghe Guo^a, Fei Yang^b, Chao Li^a, Yufei Zhao^c, Jing Qu^d, Kun Li^{a,*}, Yan Liu^{a,*}, Lili Wang^a, Lingguo Bu^d^a School of Mechanical and Electrical Engineering, Shandong Jianzhu University, Jinan 250000, China^b Shandong Labor Vocational and Technical College, Jinan 250022, China^c School of Engineering Medicine, Beijing Advanced Innovation Center for Biomedical Engineering, Beihang University, Beijing 100083, China^d Joint SDU-NTU Centre for Artificial Intelligence Research (C-FAIR), Shandong University, Jinan 250101, China

ARTICLE INFO

Article history:

Received 6 March 2025

Revised 1 June 2025

Accepted 12 June 2025

Available online 1 July 2025

Keywords:

Exoskeleton

Underactuation

Hand function impairment

Performance evaluation

ABSTRACT

In recent years, the number of stroke patients worldwide has been steadily increasing, with approximately 70% of survivors experiencing upper limb dysfunction, particularly severe impairment of fine motor skills in the hand. This limitation significantly reduces patients' ability to perform daily activities and increases the burden on both families and society. Existing hand rehabilitation exoskeletons suffer from issues such as complex structures, high production and usage costs, and limited application scenarios. This paper presents a flexible and portable hand rehabilitation robotic device based on the anatomical structure and movement characteristics of the human hand. First, a flexible exoskeleton glove based on underactuation is designed to accommodate various finger sizes. The portable device allows for rehabilitation in both hospital and home environments. Second, Adams simulation is used to verify the structural feasibility of the designed exoskeleton. Finally, device testing is performed on subjects to assess the assistive performance and motor dexterity of the hand exoskeleton using joint angle similarity tests, object grasping experiments, and force distribution tests. The experimental results show that the hand exoskeleton prototype can assist finger joints in achieving significant flexion and extension movements. Moreover, by adjusting the driving forces at each joint, it can stabilize the grasping of objects with different sizes, providing a high level of motion assistance in daily object grasping and finger joint movements. This study offers a practical and feasible technological path to reduce disability rates and improve the quality of life for patients with hand dysfunction following a stroke.

© 2025 The Author(s). Published by Elsevier B.V. on behalf of Shandong University. This is an open access article under the CC BY-NC-ND license (<http://creativecommons.org/licenses/by-nc-nd/4.0/>).

1. Introduction

Stroke, a global public health challenge, poses a serious threat to human life and health due to its high incidence, disability rate, and mortality rate [1]. According to the latest data from the World Health Organization, stroke has become the second leading cause of death worldwide. It is predicted that stroke-related mortality will increase by 50% from 2020 to 2050, with China leading this increase [2]. More alarmingly, stroke not only results in a high number of deaths but also causes long-term disabilities in many survivors, particularly the loss of hand function. This significantly impacts survivors' quality of life and social participation [3].

The loss of hand function following a stroke makes it difficult for patients to perform basic daily activities such as dressing,

eating, and writing. In severe cases, patients may even become unable to care for themselves. This loss not only causes physical pain but also has a significant psychological impact, leading to issues such as diminished self-esteem and social isolation [4].

To improve the rehabilitation outcomes of stroke patients and enhance their quality of life, the medical field has been actively exploring effective treatment methods. In recent years, with the rapid development of robotic technology, hand rehabilitation robots have gradually emerged as a promising therapeutic tool, attracting widespread attention [5]. Hand rehabilitation robots offer personalized rehabilitation programs through precise force control and motion trajectory planning, effectively promoting the recovery of hand function [6]. Existing hand rehabilitation exoskeletons can be primarily divided into two types: flexible hand exoskeletons and rigid hand exoskeletons [7].

Flexible hand exoskeletons are designed using compliant materials. For example, Mohammadi et al. [8] developed a design using flexible TPU to 3D print the compliant components for tendon-driven finger actuators. While this enhanced compliance

* Corresponding authors.

E-mail addresses: likun@sdjzu.edu.cn (K. Li), liuyan23@sdjzu.edu.cn (Y. Liu).

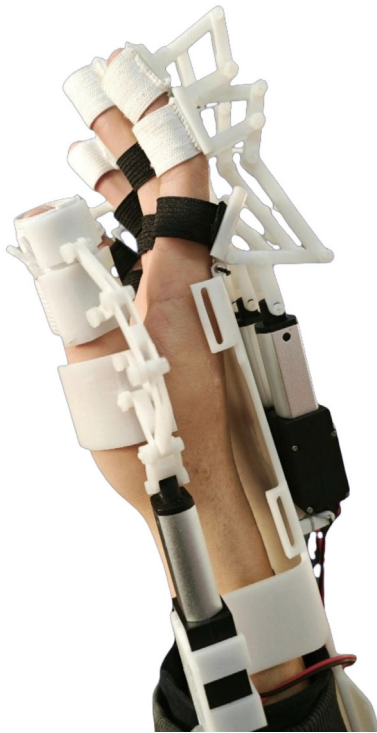


Fig. 1. Hand exoskeleton platform.

improves the fit between the hand and the exoskeleton, it results in lower precision in driving finger movements. Zhang et al. [9] designed a hand rehabilitation glove featuring segmented soft actuators with bending and stretching modules, allowing for independent or coupled motion of finger joints. Although soft hand exoskeletons have certain advantages in terms of comfort, safety, and portability [10], the materials and drive methods used result in relatively low maximum assistive forces. In particular, soft exoskeletons struggle to provide precise actuation of individual finger joints, making it difficult to achieve accurate joint assistance.

Rigid hand exoskeletons, based on traditional mechanical structures, are typically made from high-strength composite materials. Compared to soft hand exoskeletons, rigid exoskeletons provide notable advantages in force output and precise control. For instance, Marconi et al. [11] introduced the HandeXos-Beta (HX- β), a novel finger-thumb exoskeleton employing a series elastic actuator (SEA) architecture, enabling independent control of thumb flexion/extension and opposition movements (thumb-to-finger), which allows for various natural and functional grip configurations. However, the use of Bowden cables introduces nonlinear friction, which significantly reduces the wearability and efficiency of the device. Yang et al. [12] designed a portable hand rehabilitation device with a modular rack-and-pinion transmission, effectively increasing the range of motion of the index and middle fingers from 0.3° and 0.6° to 58.6° and 74.4° , respectively, helping patients recover hand function. However, the design is complex, with significant obstacles in the transmission mechanisms. The overall weight of the device is substantial, making it difficult to wear and limiting its widespread use.

Underactuated mechanisms in rigid hand exoskeletons, offer advantages in finger adaptability, assistive capabilities, and portability. For example, Lorenzo et al. [13] developed a hand exoskeleton prototype using a modular design with a single drive unit that

used an underactuated mechanism to assist finger joint movement. Birouaş et al. [14] proposed a new asymmetric underactuated robotic hand exoskeleton that used a rigid structure combining with both pulley-cable transmission and Bowden cable transmission. Each finger was controlled by a separate actuator, leveraging the natural compliance of the human body to achieve both symmetrical and asymmetrical movements. However, these underactuated exoskeletons struggle to adapt to different finger sizes, significantly weakening the assistive capability of finger joints. Although they reduce the number of actuators, the size and arrangement of these actuators affect overall portability.

In this study, a hand exoskeleton based on an underactuated structure is proposed, as shown in Fig. 1. The design utilizes a single motor to achieve multi-joint coordinated movement for a single finger. Additionally, an underactuated structural framework with a distributed pushrod motor layout is adopted to develop a low-cost, portable manufacturing solution. A multi-dimensional verification system is constructed, comprising Adams simulation, dynamic testing with Flex sensors, Brunnstrom's graded gripping experiments and force distribution tests. This system provides a comprehensive validation process, from the initial analysis of the exoskeleton to the actual product fabrication, offering a model that combines both structural rigor and functional practicality for hand rehabilitation exoskeletons.

2. Related methods

2.1. Anatomical structure and motor characteristics of fingers

The exoskeleton design must align with the anatomical structure of the human hand to ensure effective wearability. The hand consists of the thumb, index finger, middle finger, ring finger, and little finger. The thumb includes the proximal metacarpophalangeal (MP) joint and the distal interphalangeal (IP) joint, offering three degrees of freedom. For the other four fingers, the proximal metacarpal interphalangeal (MCP) joint has two degrees of freedom, while the middle interphalangeal (PIP) and distal interphalangeal (DIP) joints each have one degree of freedom, for a total of four degrees of freedom [15]. Since the anatomical structures of the middle, ring, and little fingers are similar to those of the index finger, except for differences in joint length, the joint structure of the index finger is analyzed in detail.

The index finger's skeletal structure consists of the DIP, PIP, and MCP joints, enabling flexion, extension, and abduction/adduction movements in daily activities. It also cooperates with the other fingers to perform tasks such as grasping [16]. Due to the complexity of finger joint structures and the coupling effect of joint movements (for example, when the MCP joint moves, the PIP joint also experiences some degree of flexion), the analysis of finger joints is simplified to focus primarily on extension and flexion actions.

By using a motion capture system, the movement of the finger joints is recorded to establish a basis for the exoskeleton design. As shown in Fig. 2, the PIP joint, with a peak flexion angle of approximately 120° , is the most mobile joint of the index finger. The MCP joint's range of motion is the second largest, with a peak flexion angle of around 80° , providing stability during finger movements. The DIP joint has the smallest range of motion, with a peak flexion angle of approximately 40° . The flexion angles of the three joints exhibit asynchronous changes, indicating that the exoskeleton must possess dynamic response capabilities to match the natural movement rhythm.

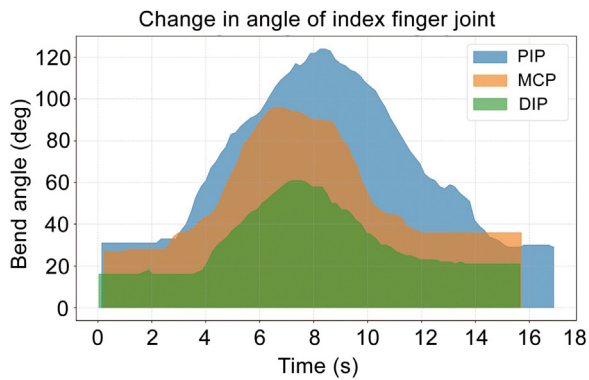


Fig. 2. Motion capture of index finger joint angle changes.

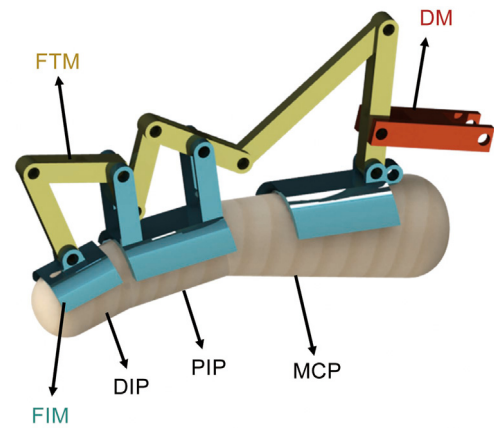


Fig. 3. Index finger structural modules.

2.2. Exoskeleton mechanical structure design

To meet the requirements for portability and flexibility, the exoskeleton adopts an underactuated design. The proposed device can be classified as a rigid, bidirectional-driven hand exoskeleton. Therefore, the device features a rigid motion chain capable of actively driving finger flexion and extension. Additionally, the rigidity indicates that the exoskeleton is made from durable materials such as metal or hard plastic. By enhancing the overall integration of the hardware system, a single motor can drive the motion trajectory of multiple joints in a single finger [17], allowing for adaptability to various object shapes and providing the compliance necessary to resist external forces. To meet the design requirements of the underactuated structure, the exoskeleton joints are developed as follows to optimize performance and efficiency.

Although the index, middle, ring, and little fingers vary in size, their skeletal structures are similar, allowing for a uniform drive structure. Taking the index finger as an example, the entire finger is modeled as a four-bar mechanism [18] with four degrees of freedom. The MCP joint has two degrees of freedom: flexion/extension and abduction/adduction. To simplify the mechanical structure of the hand exoskeleton, only the flexion/extension function of the MCP joint is retained. The finger mechanism follows the single-segment principle, such that there is an interaction point between the mechanism and the corresponding finger bones. For the index finger, these interaction points are located at three positions: the proximal phalanx, middle phalanx, and distal phalanx. The distribution of these interaction points ensures that the coordinated motion of the three phalanges provides optimal execution of fine movements and forceful grips.

To maintain simplicity and adaptability, the index finger mechanism's motion chain is designed with a single drive mode. The distances between components are determined based on user anthropometric data. As shown in Fig. 3, the wearable portion of the index finger exoskeleton consists of three main modules: the drive module (DM), the force transmission module (FTM), and the fingertip interaction module (FIM). The drive module is connected to a pushrod motor, which generates force transmitted through the force transmission module. This force is then directed to the fingertip interaction module, guiding the corresponding finger joint through flexion and extension.

In this study, the finger mechanism has been optimized compared to the exoskeletons developed by Akgun et al. [19] and Hernández et al. [20]. The force transmission module is sequentially integrated into the motion chain using screws and nuts, while flexible linkages are implemented to prevent force transmission components from following a rigid path in underactuated

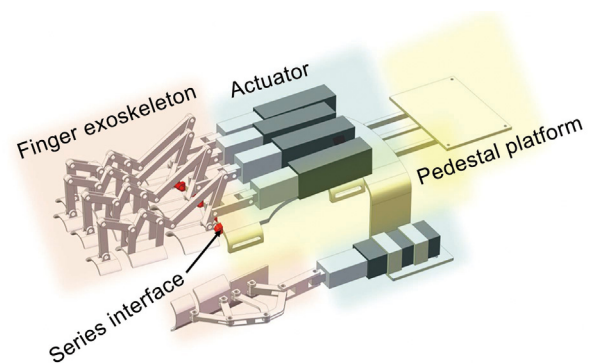


Fig. 4. Overall assembly diagram of exoskeleton.

mode. This enhances the system's adaptability to interactions between users and the device. Moreover, the flexible linkages design maintains strength while minimizing unnecessary friction and resistance, thereby improving the system's response speed and precision. This design allows the finger joints to flex and extend naturally when executing complex movements.

As shown in Fig. 4, each finger module is fixed to the base platform. When designing the finger base platform, ergonomic principles are fully considered. Extensive anthropometric data are used to ensure a close fit to the user's hand and to prevent unnatural movements caused by mechanical constraints. Additionally, the driving device is securely connected, and an elastic material cable is used to ensure a firm yet flexible attachment between the finger module and the base platform. This connection method maintains the attachment's strength while allowing for slight adjustments in the finger module's position within a certain range. Combined with the flexible underactuated structure, this design adapts to variations in hand sizes and shapes, ensuring an optimal wearing experience for each user [21]. Moreover, this connection helps absorb external shock forces, reducing potential damage to both the finger module and the base platform.

2.3. Drive unit

As mentioned earlier, each finger mechanism is designed for independent actuation. Based on the portable design concept and underactuated structure, motor-driven actuation is the optimal choice. To ensure portability, the motor size is kept as small as possible. Using Adams simulation, the displacement of the motor connection components (the red parts in Fig. 3) was analyzed

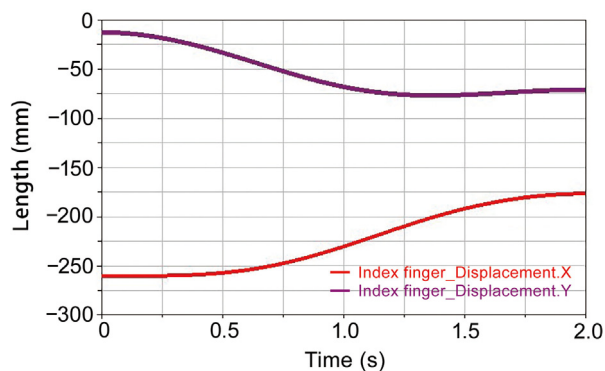


Fig. 5. Displacement of the index finger motor connector in the x and y directions.

when the exoskeleton for the index finger and thumb reached their extreme positions, as shown in Fig. 5. This figure illustrates the displacements of the index finger exoskeleton and motor connection components in both the x and y directions.

Applying the Pythagorean theorem, the linear distance between the initial and final positions was calculated as 23 mm. However, due to the slight curvature of the actual motion trajectory, the pushrod motor's stroke must exceed 23 mm. Considering the actual motor characteristics, a pushrod motor with a stroke of 30 mm was selected to accommodate this requirement.

According to the driving characteristics of the linear push rod motor, a special driving board is designed to control motor operation, as shown in Fig. 6. The drive system converts 220 V AC input voltage to a constant 12 V DC power supply. The low voltage circuit is then allocated to two parallel sub-circuits: one for the STM32F407VET6 microcontroller unit (MCU) and the other for the motor. The driver board uses RS-232 communication to control the motor. First, serial communication is performed using Python pyserial library. The USB to RS-232 signal cable connects the host and control board to ensure reliable data transmission. The control board then parses the serial data received from the host computer. Using the RS-485 protocol, it sends extension and retraction commands to the linear actuator to precisely control the exoskeleton's movement. For multi-finger cooperative operations, the movement of each finger is identified by a specific command code. By adjusting these instruction codes, various complex finger movements can be realized to illustrate the overall driving process of the exoskeleton.

2.4. Prototype exoskeleton

Based on the design concept and simulation analysis, the exoskeleton device has been validated to exhibit good motion performance. Consequently, each component was fabricated using 3D printing technology. ABS, widely used in the automotive, electronics, and other industries, was selected as the printing material. ABS is known for its excellent impact resistance, rigidity, wear resistance, chemical corrosion resistance, and ease of processing, making it a cost-effective and versatile choice [22]. Moreover, this manufacturing method results in a lightweight device, aligning well with requirements for portability and low-cost production [23].

The joints between the linkages, as well as the connections between the linkages and the finger sleeves, are secured using 3D-printed screws and nuts. During operation, the fingers fit closely within the exoskeleton, allowing for efficient motion tracking, which is crucial for effective rehabilitation. To ensure a secure fit, an elastic band is installed beneath the exoskeleton

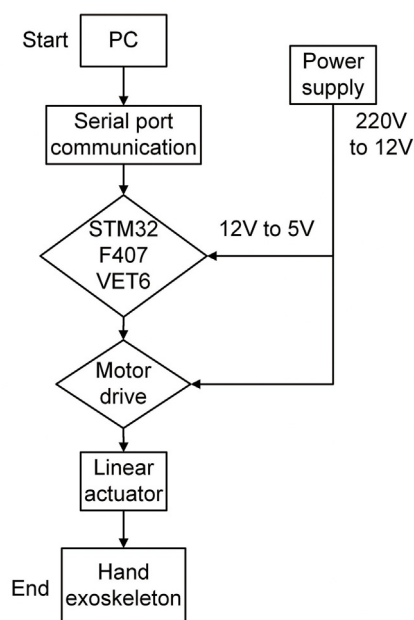


Fig. 6. Exoskeleton actuation process.

finger sleeve. When the finger is inserted, the elastic band tightens to hold the finger firmly in place [24], thereby preventing detachment or slippage during movement.

The complete hand exoskeleton consists of five finger exoskeletons attached to a backplate. The thumb is mounted on the side of the backplate, while the remaining four fingers are positioned on top. A pushrod motor is placed on the side of the backplate to drive the thumb, while four additional pushrod motors are positioned above to drive the remaining fingers. Through the coordinated operation of multiple motors, the pushrods extend and retract to assist finger flexion and extension. This overall design layout not only simplifies the structural configuration and improves integration but also enhances flexibility and operational efficiency.

3. Experimental results and analysis

3.1. Structural feasibility analysis

To verify the motion feasibility of the designed exoskeleton, an analysis was performed on the prototype to evaluate the rotational angles of the exoskeleton's joints. Adams simulation software was used for verification, in which a simplified finger model was created to drive the exoskeleton [25]. During the simulation, the angle changes between exoskeleton linkages were recorded.

As shown in Fig. 7, point A represents the MCP joint of the index finger, point B represents the PIP joint, and point C represents the DIP joint. To achieve natural finger flexion and extension movements, the following drive functions were set for each joint of the index finger: the MCP joint was driven by STEP (time, 0, 0, 2, 30d), the PIP joint by STEP (time, 0, 0, 2, 80d), and the DIP joint by STEP (time, 0, 0, 2, 80d). The finger joints followed the prescribed drive functions and moved to the final positions A, B', and C'. During this movement, the measured angles 1, 2, 3, 4, and 5 also changed as the finger flexed, reaching positions 1', 2', 3', 4', and 5'. The angle changes measured were: 57° for angle 1, 18° for angle 2, 40° for angle 3, 38° for angle 4, and 61° for angle 5.

The measurement results obtained through Adams simulations, as shown in Fig. 8, indicate that during the finger flexion

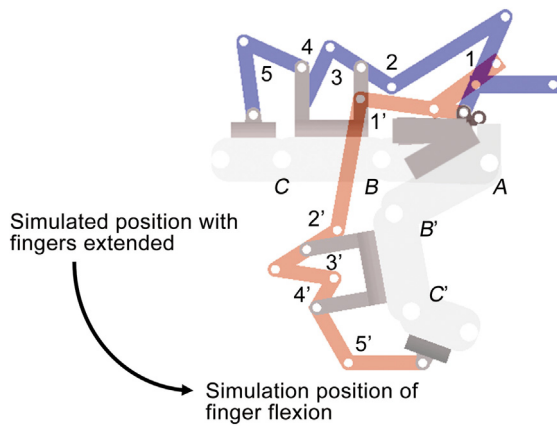


Fig. 7. Simulation position changes of the index-finger exoskeleton.

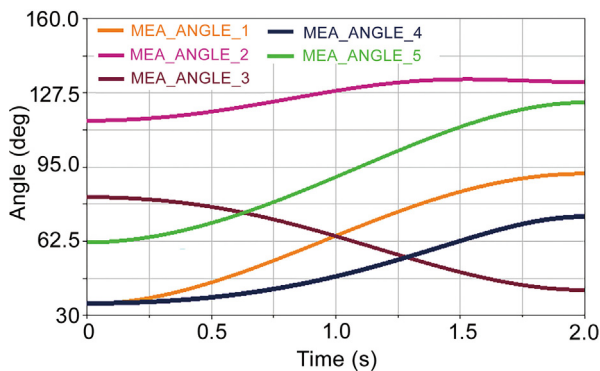


Fig. 8. Angle changes between index finger exoskeleton rods.

movement while wearing the exoskeleton, the angles between the linkages remain within reasonable ranges. No interference between structures or other issues that could affect the structural feasibility were observed during the simulation, confirming that the overall structural design meets the operational requirements.

In terms of practical validation, the simulation results show that the exoskeleton can accurately replicate the joint movement range of a healthy hand. The successful fabrication of the physical prototype demonstrates the potential of 3D printing technology in such projects. Additionally, joint angle measurements from users and object grasping experiments further confirm the device's excellent performance in assisting finger flexion/extension and executing daily tasks.

3.2. Motion similarity test

A motion similarity test was conducted to quantify the similarity of movements with and without the exoskeleton [26]. Volunteers were recruited to perform joint angle tests under two scenarios: not wearing the exoskeleton and wearing the exoskeleton. Flex2.2 angle measurement sensors were used to measure the joint angles of the fingers. These sensors cause a change in resistance when bent, which in turn results in a change in voltage. The sensors were connected to the STM32C8T6 development board, which converted the acquired resistance-based analog signals into digital signals. These signals were transmitted to the PC via a serial communication protocol for real-time display and data collection. Angle change data was collected at 50 ms intervals. During the measurement, only one joint was measured at a time to ensure more accurate results.

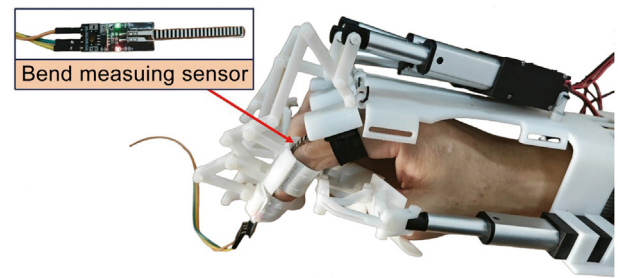


Fig. 9. Finger joint angle measurement.

As shown in Fig. 9, the experimenter was a healthy 23-year-old male wearing the exoskeleton. The test subjects were instructed to keep their fingers completely relaxed during the exoskeleton-assisted movement, allowing for purely passive movement to evaluate the exoskeleton's assistance performance on finger joints in real-world scenarios [27]. During the entire measurement process, the angle measurement sensors were attached to the back of the finger joints. The subjects then wore the exoskeleton, which assisted their flexion–extension movements. In the case without the exoskeleton, the angle sensors were fixed to the back of the corresponding finger joints using adhesive tape, and the test subjects were asked to perform natural flexion and extension movements of their fingers.

The results of the motion similarity test were shown in Fig. 10. When wearing the exoskeleton, the range of motion for each finger joint was relatively small. Among these, the difference in the DIP joint's range of motion between the exoskeleton-wearing and non-wearing conditions was the smallest, only 25°. The difference in the PIP joint's range of motion was 32°, and the MCP joint showed the largest difference, reaching 56°. However, by calculating the joint angle similarity using formula (1), the joint angle similarity was 74.19% for the PIP joint, 59.02% for the DIP joint, and 41.67% for the MCP joint. Based on these measurements, it can be concluded that the designed exoskeleton can assist finger flexion and extension to a certain extent, particularly for the PIP joint of the index finger, which showed significant joint angle changes during flexion and extension. This confirms the exoskeleton's role in finger rehabilitation and assistance.

Lower joint-angle similarities can be attributed to the space occupied by the Velcro used to secure the exoskeleton on the hand, as well as the limitations of the underactuated structure's force transmission, which reduces the effective range of motion. However, the essence of the motion was preserved, and the nature of the movement trajectory was not significantly affected. The device does not alter the natural coordinated movement of the finger joints, indicating that the exoskeleton does not negatively impact the movement.

$$\text{Similarity} = \frac{\text{Wearing exoskeleton joint angle}}{\text{Unworn exoskeleton joint angle}} \times 100\% \quad (1)$$

3.3. Fetching ability test

To ensure the effectiveness of hand rehabilitation devices, selecting appropriate and targeted training exercises to assist in-patient rehabilitation is crucial. The training program was designed based on Brunnstrom's Six-Stage Theory, which is widely accepted in the rehabilitation field. This theory classifies muscle tone and improves abnormal movements through stages [28]. It provides a method to induce responses using different movement patterns. After correcting and guiding these responses, patients can distinguish helpful movements and perform more complex

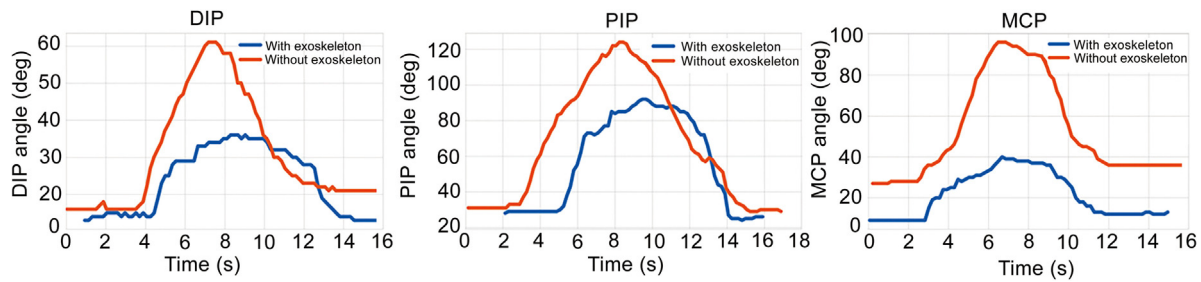


Fig. 10. Comparison of index finger joint angle change.

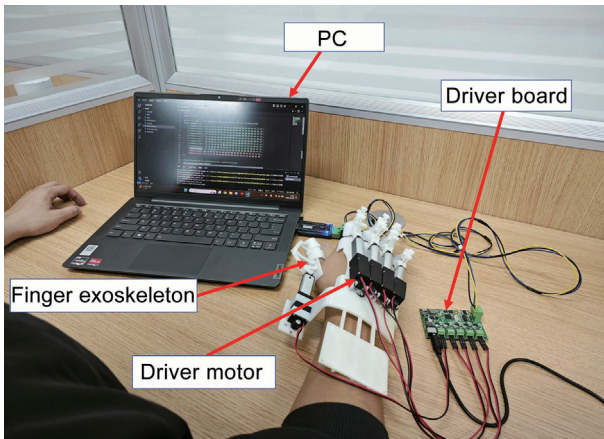


Fig. 11. Object grasping experiment.

Table 1
Personal information of testers.

Tester ID	Age	Genders	Degree of injury
1	24	Male	Non-injury
2	26	Male	Non-injury
3	20	Male	Non-injury
4	21	Male	Non-injury
5	23	Male	Non-injury

actions to achieve rehabilitation goals [29]. However, the complexity of hand movements reduces rehabilitation effectiveness and increases repetitive work. As a key step, movement categories should be completed first. It is worth noting that full-range flexion and extension of all fingers should be based on random movements of individual fingers [30]. Therefore, grasping cylindrical, spherical, and square objects were selected as experimental tasks. Grasping tasks like ball grabbing, pen grabbing, cup grabbing, and square box grabbing were chosen as rehabilitation training exercises. The experimental platform is shown in Fig. 11.

In order to assess the usability and effectiveness of the device, we recruited five male students aged 20–26 (mean = 22.8). Personal information is shown in Table 1. Informed consent was obtained from all participants. The experiment consisted of four tasks as shown in Fig. 12: grasping a ping pong ball, grasping a water cup, pinching a signing pen, holding a square box. After completing the tasks, we administered relevant questionnaires to the five healthy participants. They answered questions regarding their experiences, and we selected key items from several established surveys to complete the assessment. From the Childs Fatigue Scale (CFQ 11), we selected Q3 and Q7 to assess fatigue. From the System Usability Scale (SUS), we selected Q3 and Q4 to assess usability. From the State of Comfort Scale (GCQ), we chose Q9 and Q13 to measure the level of comfort during the use of the equipment. The GCQ is based on a four-point scale

Table 2
Questionnaire question selection.

Question number	Question
CFQ_11_Q3	Do you feel sleepy?
CFQ_11_Q7	Do you feel weak?
SUS_Q3	I think this product/website is easy to use.
SUS_Q4	I feel like I need someone with experience to help me with this product/website!
GCQ_Q9	I'm in so much pain, I can't stand it.
GCQ_Q13	I don't feel well now.

(1–4), while the remaining questions are based on a five-point scale (1–5), with higher scores indicating greater agreement with the statement. The details are shown in Table 2. The results of the questionnaire are shown in Fig. 13. The subjects did not experience any significant fatigue during device use, and reported satisfactory levels of comfort and usability.

Under the exoskeleton-wearing condition, grasping tasks were performed. As shown in Fig. 12, the four tasks were as follows: grasping a ping-pong ball, grasping a cup, pinching a pen, and grabbing a square box. The exoskeleton-assisted grasping experiments showed that the system exhibited good adaptability and flexibility in grasping objects of different shapes, sizes, and weights [31]. Notably, when grasping larger objects, the exoskeleton continued to exert force after the fingers contacted the object, resulting in better performance in grasping larger objects compared to smaller ones. The entire motion process demonstrated good stability, further validating the effectiveness of hand function assistance. It also demonstrated the robot's ability to assist with activities of daily living, thereby meeting patients' functional rehabilitation training needs.

The Six-Stage Theory was translated into quantifiable grasping training tasks. The joint angle similarity test results showed that after wearing the device, the PIP joint range of motion reached 74.19%, close to the clinically effective threshold of 75% reported by Kabir et al. This was attributed to the efficient force transmission characteristics of the rigid linkage structure. These findings provide data support for establishing a rehabilitation assessment system based on biomechanical parameters.

3.4. Joint force distribution test

Force distribution tests were performed using FSR thin film pressure sensors to quantify the forces applied to the various joint areas of the index finger while wearing the exoskeleton. Measurements of the index finger joints were made using FSR pressure sensors, which produce a corresponding change in resistance value when the FSR sensor receives a change in pressure, which causes a change in the voltage signal [32]. The analog signal of the collected resistance value is converted into a digital signal,

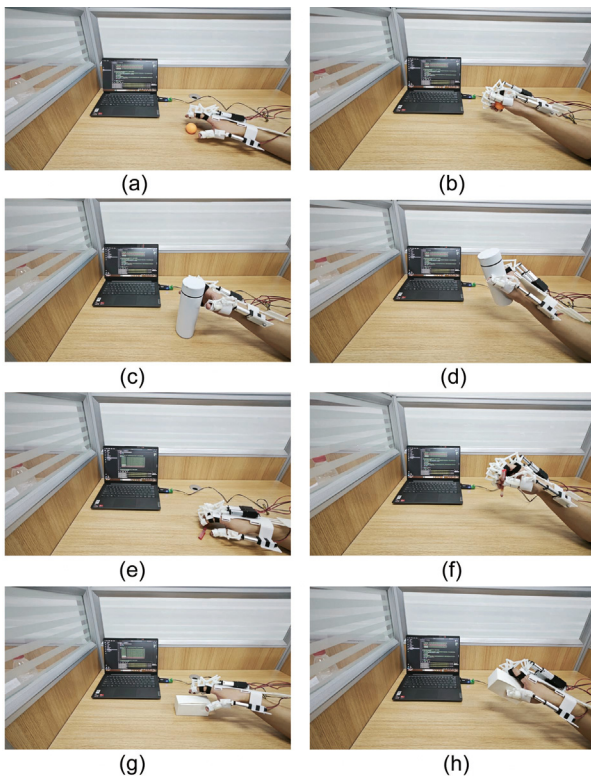


Fig. 12. Wear the exoskeleton to grasp a variety of objects. (a) Spherical-object (no touch). (b) Spherical-object (touch). (c) Cup-object (no touch). (d) Cup-object (touch). (e) Pen-object (no touch). (f) Pen-object (touch). (g) Square-object (no touch). (h) Square-object (touch).

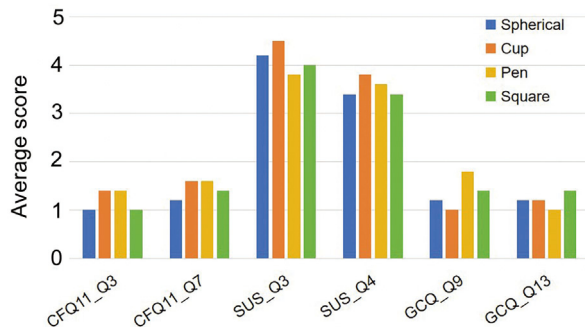


Fig. 13. Questionnaire results.

which is transmitted to a PC through a serial communication protocol for real-time display and data acquisition. Angle change data are acquired at 50 ms intervals. Only one joint is measured at a time to obtain more accurate measurements. The FSR pressure sensor (RP-C10-ST) is attached to the surface of the object to be gripped, as shown in the Fig. 14. The resulting pressure values form a time series.

A healthy male, aged 23, was selected for the experiment. The experimenter wore the exoskeleton and held his hand in a relaxed position near a bottle-shaped object bearing the sensor. When the exoskeleton assisted the index finger's flexion, the relevant joints contacted the FSR sensor to generate pressure signals. In each trial, we carefully aligned the targeted joint with the sensor to ensure measurement accuracy.

The pressure signal is shown in Fig. 15. The load at the DIP joint is the largest at 5.6 N, followed by 5.2 N at the PIP joint, while the MCP joint load was the smallest at 4.1 N. This is

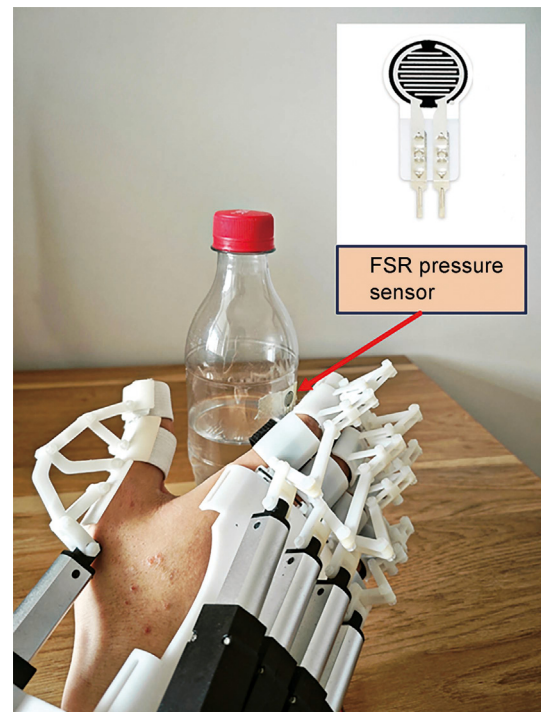


Fig. 14. Force distribution experiment.

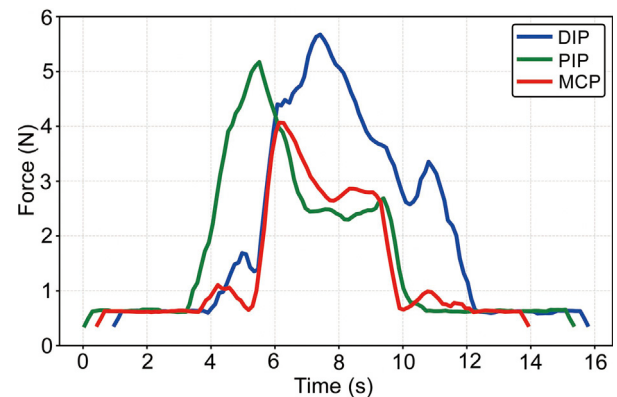


Fig. 15. Changes in pressure signals at each joint.

related to the underactuated structure of the exoskeleton, which prioritizes the force output to the distal structure to ensure that the grasping force exists to satisfy the function of object grasping. Therefore, the data suggest that the exoskeleton's force transmission path tends to favor the mid-distal end, which not only significantly aids object-grasping assistance, but also possesses sufficient driving force for the rehabilitation movement of the finger joints.

4. Conclusion

This study integrates an underactuated mechanism based on the physiological structure of the human hand to develop a hand rehabilitation exoskeleton system with practical value. It aims to provide efficient, personalized rehabilitation training for stroke patients and other individuals with impaired hand function. Compared to existing research, this device achieves breakthroughs in three key areas. First, the design of a single motor-driven mechanism enables multi-joint coordinated movement of a single finger

while reducing the number of actuators without compromising movement precision. Second, the use of an elastic band combined with an ABS material composite structure ensures comfort while keeping the device lightweight. Finally, the ergonomic modular design expands the range of finger size adaptation.

While this study has achieved a series of positive outcomes, some limitations remain. First, the underactuated mechanism results in a range of motion for the DIP joint limited to only 59.02%. Although the underactuated structure allows multi-degree-of-freedom motion, joint coupling effects can reduce assistance. For example, the MCP joint receives only 4.1 N of driving force, while the PIP and DIP joints receive 5.2 N and 5.6 N, respectively, which may lead to uneven force distribution. Additionally, the fit of the exoskeleton for fingers of different sizes needs improvement to accommodate a broader population. In light of these limitations, future work will focus on the following aspects: First, to optimize the exoskeleton mechanism design and to explore more precise driving methods and control algorithms to enhance assistive performance. Second, to increase the sample size and to conduct long-term controlled clinical trials to gather more data on different patient groups' experiences.

In conclusion, the hand rehabilitation exoskeleton robot proposed in this study holds significant theoretical importance and broad application prospects. However, it still requires continuous improvement to meet the growing demand for rehabilitation.

CRedit authorship contribution statement

Lei Zhao: Project administration. **Fenghe Guo:** Writing – original draft. **Fei Yang:** Investigation. **Chao Li:** Data curation. **Yufei Zhao:** Formal analysis. **Jing Qu:** Data curation. **Kun Li:** Formal analysis. **Yan Liu:** Validation. **Lili Wang:** Resources. **Lingguo Bu:** Supervision, Conceptualization.

Declaration of competing interest

The authors declare that they have no known competing financial interests or personal relationships that could have appeared to influence the work reported in this paper.

Acknowledgments

This work was supported in part by the National Natural Science Foundation of China (52302500, 52205275), in part by the Natural Science Foundations of Shandong Province, China (ZR2021QE115, ZR2022QE297, ZR2020ME115, and ZR2023QF119).

Appendix A. Supplementary data

Supplementary material related to this article can be found online at <https://doi.org/10.1016/j.birob.2025.100248>.

References

- [1] S.J.X. Murphy, D.J. Werring, Stroke: causes and clinical features, *Medicine* 48 (9) (2020) 561–566.
- [2] V.L. Feigin, et al., World stroke organization (WSO): Global stroke fact sheet 2022, *Int. J. Stroke* 17 (1) (2022) 18–29.
- [3] R. Ranzani, et al., Neurocognitive robot-assisted rehabilitation of hand function: a randomized control trial on motor recovery in subacute stroke, *J. NeuroEng. Rehabil.* 17 (1) (2020) 115.
- [4] R. Kabir, M. Sunny, H. Ahmed, M. Rahman, Hand rehabilitation devices: A comprehensive systematic review, *Micromachines* 13 (7) (2022) 1033.
- [5] T. Du Plessis, K. Djouani, C. Oosthuizen, A review of active hand exoskeletons for rehabilitation and assistance, *Robotics* 10 (1) (2021) 40.
- [6] J. Wang, J. Zheng, Y. Zhao, K. Yang, Structure design and coordinated motion analysis of bionic crocodile robot, *Biomim. Intell. Robot.* 4 (2) (2024) 100157.
- [7] Y. Zhu, W. Gong, K. Chu, X. Wang, Z. Hu, H. Su, A novel wearable soft glove for hand rehabilitation and assistive grasping, *Sensors* 22 (16) (2022) 6294.
- [8] S. Bai, M.R. Islam, V. Power, L. O'Sullivan, User-centered development and performance assessment of a modular full-body exoskeleton (AXO-SUIT), *Biomim. Intell. Robot.* 2 (2) (2022) 100032.
- [9] Z. Zhang, A. Calderon, X. Huang, G. Wu, C. Liang, Design and driving performance study of soft actuators for hand rehabilitation training, *MDER* 17 (2024) 237–260.
- [10] J. Lai, A. Song, K. Shi, Q. Ji, Y. Lu, H. Li, Design and evaluation of a bidirectional soft glove for hand rehabilitation-assistance tasks, *IEEE Trans. Med. Robot. Bionics* 5 (3) (2023) 730–740.
- [11] D. Marconi, A. Baldoni, Z. McKinney, M. Cempini, S. Crea, N. Vitiello, A novel hand exoskeleton with series elastic actuation for modulated torque transfer, *Mechatronics* 61 (2019) 69–82.
- [12] L. Yang, F. Zhang, J. Zhu, Y. Fu, A portable device for hand rehabilitation with force cognition: Design, Interact. Exp. *IEEE Trans. Cogn. Dev. Syst.* 14 (2) (2022) 599–607.
- [13] L. Bartalucci, et al., An original mechatronic design of a kinaesthetic hand exoskeleton for virtual reality-based applications, *Mechatronics* 90 (2023) 102947.
- [14] F.I. Birouaş, R.C. Țarcă, S. Dzitac, I. Dzitac, Preliminary results in testing of a novel asymmetric underactuated robotic hand exoskeleton for motor impairment rehabilitation, *Symmetry* 12 (9) (2020) 1470.
- [15] J.B. Tang, Rehabilitation after flexor tendon repair and others: a safe and efficient protocol, *J. Hand. Surg. Eur.* 46 (8) (2021) 813–817.
- [16] P. Li, Y. Deng, X. Guo, J. Wang, Nursing effects of finger exercise on cognitive function and others for cerebral ischemic stroke patients, *Am. J. Transl. Res.* 13 (4) (2021) 3759–3765.
- [17] V. Moreno-Sanjuan, A. Císnal, J.-C. Fraile, J. Pérez-Turiel, E. de-la Fuente, Design and characterization of a lightweight underactuated RACA hand exoskeleton for neurorehabilitation, *Robot. Auton. Syst.* 143 (2021) 103828.
- [18] G. Carbone, Numerical and experimental performance estimation for a ExoFing - 2 DOFs finger exoskeleton, *Robotica* 40 (6) (2022) 1820–1832.
- [19] G. Akgun, A.E. Cetin, E. Kaplanoglu, Exoskeleton design and adaptive compliance control for hand rehabilitation, *Trans. Inst. Meas. Control* 42 (3) (2019) 493.
- [20] C. Hernández-Santos, Y.A. Davizón, A.R. Said, R. Soto, L.C. Félix-Herrán, A. Vargas-Martínez, Development of a wearable finger exoskeleton for rehabilitation, *Appl. Sci.* 11 (9) (2021) 4145.
- [21] E. Amirpour, et al., A novel hand exoskeleton to enhance fingers motion for tele-operation of a robot gripper with force feedback, *Mechatronics* 81 (2022) 102695.
- [22] F. Trauzettel, Emmanuel Vander Poorten, Mouloud Ourak, Jenny Dankelman, P. Breedveld, Six smart guidelines for high-tech manufacture on low-tech 3D printers: the case of the 3Flex, *J. Eng. Des.* 35 (6) (2024) 665–684.
- [23] R. Toshev, N. Kolatsis, A. Shamzzuzoha, P. Helo, The economics of additive manufacturing and topology optimisation – a case analysis of the electric scooter, *J. Eng. Des.* 34 (4) (2023) 313–338.
- [24] P. Agarwal, et al., A case report on enhancing the dexterity of finger prostheses through the use of a 3D-printed joint emulator, *Cureus* (2024).
- [25] Y. Wang, F. Pancheri, T.C. Lueth, Y. Sun, Design of a spider-inspired wheeled compliant leg for search mobile robots, *Biomim. Intell. Robot.* 4 (4) (2024) 100182.
- [26] N. Sun, G. Li, L. Cheng, Design and validation of a self-aligning index finger exoskeleton for post-stroke rehabilitation, *IEEE Trans. Neural Syst. Rehabil. Eng.* 29 (2021) 1513–1523.
- [27] W. Chen, et al., Soft exoskeleton with fully actuated thumb movements for grasping assistance, *IEEE Trans. Robot.* 38 (4) (2022) 2194–2207.
- [28] R. Akter, N. Sharma, S. Ahmed, A.K. Srivastav, Combined effect of Brunnstrom's hand rehabilitation and functional electrical stimulation for improving hand function in patients with chronic stroke: A randomized controlled trial, *J. Bodyw. Mov. Ther.* 35 (2023) 84–90.
- [29] E.R. Triolo, B.F. BuSha, Design and experimental testing of a force-augmenting exoskeleton for the human hand, *J. NeuroEng. Rehabil.* 19 (1) (2022) 23.
- [30] G. Lu, X. Liu, Q. Zhang, Z. Zhao, R. Li, Z. Li, Design and analysis of rehabilitation evaluation system for finger rehabilitation robot, *IJAT* 18 (5) (2024) 671–678.
- [31] M. Dragusanu, D. Troisi, A. Villani, D. Prattichizzo, M. Malvezzi, Design and prototyping of an underactuated hand exoskeleton with fingers coupled by a gear-based differential, *Front. Robot. AI* 9 (2022) 862340.
- [32] G. Abbate, A. Giusti, L. Randazzo, A. Paolillo, Learning hand state estimation for a light exoskeleton, 2024.